

# ChemComm

Accepted Manuscript



This is an *Accepted Manuscript*, which has been through the Royal Society of Chemistry peer review process and has been accepted for publication.

*Accepted Manuscripts* are published online shortly after acceptance, before technical editing, formatting and proof reading. Using this free service, authors can make their results available to the community, in citable form, before we publish the edited article. We will replace this *Accepted Manuscript* with the edited and formatted *Advance Article* as soon as it is available.

You can find more information about *Accepted Manuscripts* in the [Information for Authors](#).

Please note that technical editing may introduce minor changes to the text and/or graphics, which may alter content. The journal's standard [Terms & Conditions](#) and the [Ethical guidelines](#) still apply. In no event shall the Royal Society of Chemistry be held responsible for any errors or omissions in this *Accepted Manuscript* or any consequences arising from the use of any information it contains.



Journal Name

## COMMUNICATION

## Novel Pd–Cu–Zr hydrogen separation membrane with a high tolerance to sulphur poisoning

Received 00th January 20xx,  
Accepted 00th January 20xx

S. Nayeibossadri,<sup>a</sup> J. Speight<sup>a</sup> and D. Book<sup>a</sup>

DOI: 10.1039/x0xx00000x

www.rsc.org/

**The effects of small Zr addition (less than 2 at.%) to the fcc phase of Pd–Cu hydrogen separation alloy was investigated. Hydrogen flux variations in Pd–Cu and Pd–Cu–Zr alloys under 1000 ppm H<sub>2</sub>S+H<sub>2</sub> feed gas showed the marked effect of Zr addition for improving the resistance to the sulphur poisoning.**

Palladium-copper (Pd–Cu thereafter) is of particular interest because of the lower cost compared to Pd membrane and a degree of tolerance to the surface poisoning, notably by sulphur, exhibited by face centred cubic (fcc) structure of this alloy [1–11]. It was shown [1] that the permeability of Pd–Cu alloys is greatly influenced by the Cu content and hence, crystal structure of the alloy. An extensive phase diagram study detailing the various phases present in the Pd–Cu alloy, was performed by Subramanian and Laughlin [12].

Hydrogen flux through the body centered cubic (bcc) phase can be substantially reduced by trace impurities in the gas stream. Transition from sulphur poisoning to partial sulphur tolerance was observed with increasing temperature in the presence of 1000 ppm H<sub>2</sub>S for the Pd<sub>47</sub>Cu<sub>53</sub> alloy foil [9]. This was attributed with the alloy transition from bcc to fcc phase and specific surface characteristics of the fcc phase [9,13]. In fact, hydrogen flux through the bcc Pd<sub>47</sub>Cu<sub>53</sub> foil was undetectable within 5 minutes of exposure to 1000 ppm H<sub>2</sub>S at 350 °C [14]. X-ray Photoelectron Spectroscopy (XPS) measurement revealed that sulphur is located near to the top surface and therefore the immediate decline in the hydrogen flux may be due to the formation of a hydrogen impermeable Pd–Cu–S layer. Inhibition of hydrogen permeation by H<sub>2</sub>S was also examined for a range of Pd–Cu membranes at various H<sub>2</sub>S concentrations and temperatures [15]. At low H<sub>2</sub>S concentrations, hydrogen flux decreased as a result of blocked active surface sites for hydrogen dissociation. However, complete failure of Pd–Cu membranes at 450 °C, which was independent of exposure time, occurred at the H<sub>2</sub>S concentration of approximately 300 ppm as result of alloy sulfidation, and lattice expansion.

H<sub>2</sub>S inhibition and subsequent H<sub>2</sub> flux recovery of Pd<sub>70</sub>Cu<sub>30</sub> thin film (~2 μm) were examined at 450 °C under 2, 20 and 100 ppm H<sub>2</sub>S. A sharp decrease in hydrogen flux was observed for the exposed sample depending on H<sub>2</sub>S concentration [16]. In another study [17] the effect of H<sub>2</sub>S to H<sub>2</sub> partial pressure on the sulfidation of Pd<sub>70</sub>Cu<sub>30</sub> alloy was shown to be experimentally in a good agreement with thermodynamic calculations within the broad temperature range (77–977 °C). The H<sub>2</sub>S to H<sub>2</sub> ratios required to form Pd<sub>4</sub>S and Cu<sub>2</sub>S as the dominant sulfidation products were predicted. However, some deviations from the predicted values were observed, which was attributed to the formation of non-ideal solution of Pd–Cu alloy as a result of Cu segregation at the surface. It is known that interaction with strongly adsorbing species such as sulphur can potentially induce surface segregation [18]. Hence, formation of any sulphide phase may be accompanied by a selective segregation of the alloy constituents to the surface. This leads to the irreversible chemical and structural modification of the surface, which can ultimately cease hydrogen permeation through the alloy [19]. Nevertheless, under specific circumstances preferential segregation can be beneficial in order to mitigate the surface sulfidation. For example, Pd–Au alloy membranes have recently received increasing attention due to their higher sulphur resistance compared to many other Pd alloys [20,21,22]. It is known that sulphur tolerance is mainly induced by a higher gold concentration on the surface caused by its preferential segregation [23,24].

Therefore, adding elements with a tendency for preferential segregation may be a possible method to discourage the S–surface interaction in the Pd–Cu membranes. However, this technique may oppose the requirement for the long term stability of membranes as the preferential segregation can potentially lead to the degradation of the membrane properties [19]. In this study we seek a new strategy by stabilising the alloy structure to retard the surface segregation and possibly slow down the bulk sulphide formation kinetics.

The starting materials, palladium powder (99.9985%) and copper wire (99.9%, diameter: 1mm) were purchased from Alfa Aesar and Sigma Aldrich respectively. The starting materials were weighed and loaded into a water-cooled copper hearth within the vacuum arc furnace to produce approximately 2.5g of fcc Pd–Cu alloy buttons

<sup>a</sup>School of Metallurgy and Materials, University of Birmingham, Edgbaston, Birmingham, B15 2TT, UK  
E-mail: s.nayeibossadri@bham.ac.uk

by arc melting. The Pd–Cu alloys buttons were then cold rolled into the foil and additional element (Zr) was deposited on the foil surface using a Closed Field Unbalanced Magnetron Sputter Ion Plating (CFUBMSIP) system supplied by Teer Coatings Ltd. The weight gain of the sample was monitored to calculate the amount of the additional element. Sample was re-melted 3 times by arc melting and subsequently cold rolled to foils with a target aiming a thickness of 100 microns. The rolled foils were annealed under high vacuum ( $10^{-5}$  mbar) at 650 °C for 96 h to increase the homogeneity throughout the bulk of the membranes. X-Ray Diffraction (XRD) measurements of the foil were obtained by a Bruker D8-Advanced diffractometer using monochromatic CuK $\alpha$  radiation ( $\lambda = 1.54056$  Å). Thickness measurements of the foils and further compositional analyses on the cross section of the samples were performed using a Joel 6060 Scanning Electron Microscopy (SEM) equipped with an INCA 300 Energy Dispersive Spectroscopy (EDS). Hydrogen flux was measured using a hydrogen permeation system designed and built in the School of Metallurgy and Materials [25]. The performance of the membranes under gas stream containing H<sub>2</sub>S were examined by replacement (200 ml min<sup>-1</sup>) of the hydrogen feed to the 1000±10 ppm H<sub>2</sub>S+H<sub>2</sub> gas mixture at 450 °C purchased from BOC. The feed gas was controlled using Brooks 5850S Mass Flow Controller (MFC) calibrated over a range of 6–600 ml min<sup>-1</sup> with an accuracy of ±6 ml min<sup>-1</sup>. A constant upstream pressure of 6.18 bar was applied by continuous hydrogen flow and downstream pressure was maintained at 1 bar at all times using a back-pressure regulator to replicate the condition used in reference 1. The permeated gas flow was measured by Brooks 5850S MFC placed after the back-pressure regulator.

Table 1 shows the average atomic compositions of the annealed samples obtained from the cross sections. No substantial compositional difference was observed through the cross section of the samples, indicating the homogeneity of the samples. The compositions obtained by the EDS analyses relate to the fcc region of the Pd–Cu phase diagram [12].

The structures of Pd–Cu and Pd–Cu–Zr alloys after fabrication and following vacuum annealing were analysed by XRD in Fig. 1 (a–d). As-fabricated samples show relatively wide XRD peaks with reflection patterns corresponding to fcc structure. The Pd–Cu binary alloy as-fabricated (Fig. 1a), shows a preferential orientation along the (220) plane. Whereas XRD patterns for powdered Pd–Cu alloy with completely randomly oriented grains shows the highest peak intensity along the (111) plane [26]. Hence, the preferential orientation observed in Fig. 1a may be related to the cold rolling. Such a preferential orientation along (220) plane after fabrication is also observed in the case of Pd–Cu–Zr alloy in Fig. 1c. The structures of the same samples after annealing are shown in Fig. 1 (b and d).

Table 1: EDS analyses of the Pd–Cu Pd–Cu–Zr alloys annealed at 650 °C for 96 h.

Sample	EDS (at.%)			Thickness (μm)	Notes
	Pd	Cu	Zr		
PdCu	65.1±0.1	34.9±0.1	-	97	Fcc
PdCuZr	61±0.4	37.2±0.5	1.8±0.4	112.5	Fcc

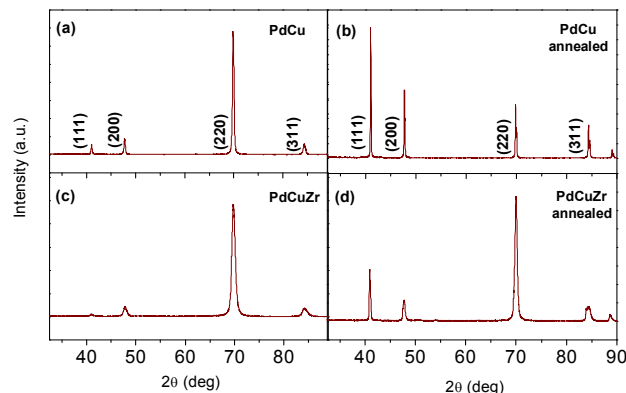


Figure 1: XRD patterns of Pd<sub>65.1</sub>Cu<sub>34.9</sub> and Pd<sub>61</sub>Cu<sub>37.2</sub>Zr<sub>1.8</sub> samples after cold rolling (a and c) and after annealing at 650 °C for 96 h under vacuum (b and d).

It can be seen that samples retain their fcc structure after annealing, whilst the XRD peaks seem to be sharper as a result of the grain growth and stress relief compared to the as-fabricated samples. Whilst, Preferential orientation along (111) plane is observed for the Pd–Cu annealed samples (Fig. 1b), the annealed Pd–Cu–Zr alloy (Fig. 1d) maintains a very similar structure to the as-fabricated state after annealing. This may imply to the structural stability of Pd–Cu–Zr sample and its resistance to the local atomic diffusion under the annealing conditions used in this study.

Figure 2 compares hydrogen permeability of the alloys in this study with the corresponding binary Pd–Cu alloys reported in the literature at 350 °C [1,3]. Excellent agreement can be seen for the hydrogen permeability of our binary Pd<sub>65.1</sub>Cu<sub>34.9</sub> alloy and the literature value. Pd–Cu–Zr membrane shows almost similar hydrogen permeability to the corresponding binary alloy although the membrane thickness is about 4 times larger than the reference data in Fig. 2.

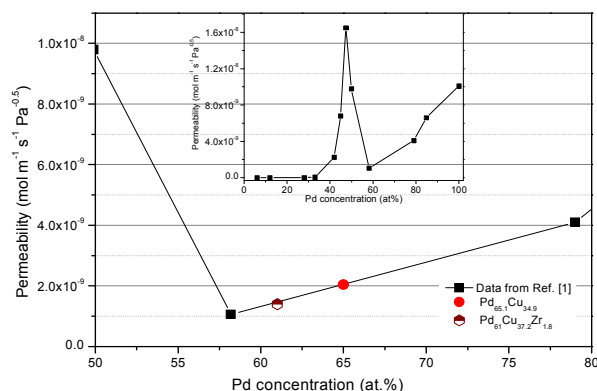


Figure 2: Comparisons between the hydrogen permeability values of Pd<sub>65.1</sub>Cu<sub>34.9</sub> and Pd<sub>61</sub>Cu<sub>37.2</sub>Zr<sub>1.8</sub> alloys with the respective binary alloys at 350 °C. The inset graph shows hydrogen permeability values of the Pd–Cu binary alloys as a function of Pd content at 350 °C. Solid line is guide for the eye.

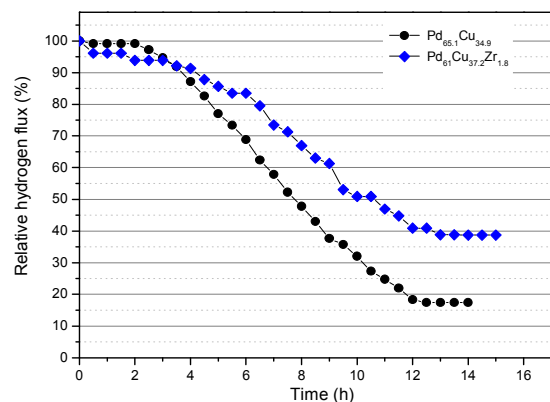


Figure 3: Sulphur poisoning of Pd<sub>65.1</sub>Cu<sub>34.9</sub> and Pd<sub>61</sub>Cu<sub>37.2</sub>Zr<sub>1.8</sub> alloys at 450 °C. The feed gas contains 1000 ppm H<sub>2</sub>S+H<sub>2</sub>.

The stability of hydrogen transport through the binary and ternary alloy membranes under hydrogen atmosphere containing 1000 ppm H<sub>2</sub>S was investigated at 450 °C. Figure 3 shows the relative hydrogen flux through the membranes when the pure hydrogen feed gas was switched to the mixture of 1000 ppm H<sub>2</sub>S+H<sub>2</sub> gas at the end of hydrogen permeation measurements. It seems that the stability of the Pd–Cu–Zr membrane is noticeably improved compared to the Pd<sub>65.1</sub>Cu<sub>34.9</sub> binary alloy.

For example, after 8 h of H<sub>2</sub>S exposure hydrogen flux reduces to 50% of its original value in the case of Pd<sub>65.1</sub>Cu<sub>34.9</sub>. In comparison, hydrogen flux through Pd–Cu–Zr alloy decreases only to 65% of its original value after similar duration of H<sub>2</sub>S exposure. Furthermore, Pd<sub>65.1</sub>Cu<sub>34.9</sub> and Pd–Cu–Zr alloys show limited hydrogen flux reductions (less than 10%) up to 3h of H<sub>2</sub>S exposure. It is known that [22,27] initial decay in the hydrogen flux of Pd–based membranes by H<sub>2</sub>S exposure occurs by a reduction in the catalytic activity of Pd as a result of adsorbed sulphur on the surface sites. However, more severe decay in the hydrogen flux results from subsequent surface growth of sulphide components layers and ultimately bulk sulfidation of the membrane. Thus, whilst the limited hydrogen flux reduction at early stages (<3h) of H<sub>2</sub>S exposure for Pd<sub>65.1</sub>Cu<sub>34.9</sub> and Pd–Cu–Zr alloys may be related to the catalytic deactivation for hydrogen dissociation on the surface of the membranes, the higher rate of hydrogen flux reduction and its complete suppression at the later stage of H<sub>2</sub>S exposure is probably related to the formation of sulphide phases with significantly lower permeability for hydrogen [27]. Therefore, the hydrogen permeability loss is expected to be irreversible at this stage. Sulfidation of Pd–Cu alloys has been shown [15,17] to be a function of H<sub>2</sub>S–H<sub>2</sub> ratio and temperature. The applied experimental conditions used in this study satisfying the thermodynamic condition [17] for the sulfidation of Pd–Cu alloys. The crystallographic structures of the samples after H<sub>2</sub>S exposure are shown in Fig. 4(a and b). Pd<sub>4</sub>S/Cu<sub>2</sub>S sulphide phases are formed after H<sub>2</sub>S exposure. Surprisingly, Pd<sub>4</sub>S phase is not the dominant observed phase in our samples as expected from thermodynamic calculations [17]. Similar effects were observed and attributed to the formation of non-ideal solid solution as a result of Cu segregations due to its high affinity to sulphur [15,17]. Here, Cu

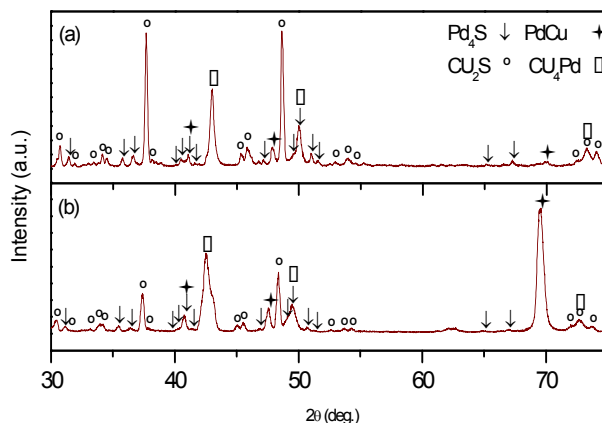


Figure 4: XRD diffraction patterns of (a) Pd<sub>65.1</sub>Cu<sub>34.9</sub> and (b) Pd<sub>61</sub>Cu<sub>37.2</sub>Zr<sub>1.8</sub> alloys after exposure to 1000 ppm H<sub>2</sub>S+H<sub>2</sub> at 450 °C.

segregation is observed for both samples leading to Cu<sub>2</sub>S phase being the dominant sulphide phase. Cu segregation is further confirmed by observation of Cu rich Cu–Pd phase/s on the top layers of the membranes. However, it should be noted that Pd–Cu–Zr ternary alloy in Fig. 4b retains its texture along (220) plane after H<sub>2</sub>S exposure, similar to the membrane behaviour observed after annealing (Fig. 1d). The structural stability of Pd–Cu–Zr alloy was suggested to originate from its resistance to the local atomic diffusion. Such behaviour may also significantly influence Cu segregation during H<sub>2</sub>S exposure, which appears to play a key role during the membranes sulfidation. Overall, it seems that sulfidation kinetics in Pd–Cu–Zr alloy reflect the structural stability of the (220) texture induced by Zr addition.

Alloying can alter the poisoning resistance in Pd–based membranes by changing the surface reactivity (chemical composition) and electronic structure of the alloy [28,29,30]. Alfonso et al. [18] showed that whilst Pd interacts more strongly with S compared to Cu, the adsorption energies in general are weaker on the alloy surfaces. Ling et al. [31] investigated the effect of Pd alloying with Cu and showed that unlike Pd, Pd<sub>75</sub>Cu<sub>25</sub> alloy has a spatially heterogeneous set of binding sites. These binding sites were geometrically similar but had varying local atomic compositions. Furthermore, the significant contribution of electronic factors for H<sub>2</sub>S adsorption on the surface of Pd and Pd alloys were suggested [18,28,29]. As a result, Zr addition may change the local atomic composition on the surface of Pd–Cu–Zr alloy by preserving the (220) texture. This may lead to the formation of new binding sites with unique energies, which change H<sub>2</sub>S adsorption preferences, thus making H<sub>2</sub>S–surface interaction less favourable. Nevertheless, the elemental segregations observed in our samples under H<sub>2</sub>S containing atmosphere, imply that the improved H<sub>2</sub>S poisoning resistance of Pd–Cu–Zr alloy may primarily originate from the observed structural stability as a result of Zr addition. In other words, we may propose that the kinetics for the surface and bulk sulfidation is sluggish as a result of decreased diffusivity of Pd and particularly Cu atoms in Pd–Cu–Zr alloy.

In summary, XRD analyses revealed that the Pd–Cu–Zr sample could retain the cold-rolled induced surface texture after annealing under vacuum at 650 °C for 96 h. This was attributed to the structural stability of this sample as a result of Zr addition. Pd–Cu–Zr sample showed greater resistance to the surface poisoning in the 1000 ppm H<sub>2</sub>S+H<sub>2</sub> atmosphere when compared to Pd<sub>65.1</sub>Cu<sub>34.9</sub> alloy, which could be related to the effect of Zr for preserving the alloy texture and influencing the surface reactivity and electronic structure of alloy surface. However, we may suggest that the primary effect of Pd–Cu–Zr sample for improved H<sub>2</sub>S resistance originates from the Zr induced structural stability at high temperatures, which can significantly slow down the Pd and Cu surface segregation, hence bulk sulfidation. This may result in development of a highly stable membrane at low to moderate H<sub>2</sub>S (<100 ppm) levels. To the best of our knowledge, this is first time the potential of Pd–Cu–Zr alloy as a hydrogen purification membrane is reported with an improved resistance to the surface poisoning by H<sub>2</sub>S.

Support from the Birmingham Science City Hydrogen Energy projects, and the Hydrogen and Fuel Cell Research Hub, is gratefully acknowledged.

## Notes and references

- 1 D.L. McKinley, *US patent* **1969**, 3, 439, 474,
- 2 F. Roa, M.J. Block, and J. D. Way, *Desalination* **2002**, 147, 411
- 3 B.H. Howard, R.P. Killmeyer, K.S. Rothenberger, A.V. Cugini, B.D. Morreale, R.M. Enick, and F. Bustamante, *Journal of Membrane Science* **2004**, 241, 207
- 4 L. Yuan, A. Goldbach, and H. Xu, *Journal of Physical Chemistry B* **2007**, 111, 10952
- 5 S.M. Opalka, W. Huang, D. Wang, T.B. Flanagan, O.M. Løvvik, S.C. Emerson, Y. She, and T.H. Vanderspurt, *Journal of alloys and Compounds* **2007**, 44, 447, 583
- 6 L. Yuan, A. Goldbach, and H. Xu, *Journal of Membrane Science* **2008**, 322, 39
- 7 L. Yuan, A. Goldbach, and H. Xu, *Journal of Physical Chemistry B* **2008**, 112, 12692
- 8 A. Goldbach, L. Yuan, and H. Xu, *Separation and Purification Technology* **2010**, 73, 65
- 9 B.D. Morreale, M.V. Ciocco, B.H. Howard, R.P. Killmeyer, A.V. Cugini, and R.M. Enick, *Journal of Membrane Science* **2004**, 241, 219
- 10 Cu–Pd–M hydrogen separation membranes, US patent, US 8608829 B1
- 11 N. Pomerantz, and Y. H. Ma, *Industrial Engineering Chemical Research*, **2009**, 48, 4030
- 12 P.R. Subramanian, and D.E. Laughlin, *Journal of Phase Equilibria* **1991**, 12, 2, 231
- 13 P. Kamakoti, B. D. Morreale, M.V. Ciocco, B.H. Howard, R.T. Killmeyer, A.V. Cugini, and D.S. Sholl, *Science* **2005**, 307, 569
- 14 C.P. O'Brien, B. H. Howard, J.B. Miller, B.D. Morreale, and A.J. Gellman, *Journal of Membrane Science* **2010**, 349, 380
- 15 A. Kulprathipanja, G.O. Alptekin, J.L. Falconer, J.D. Way, *Journal of Membrane Science* **2005**, 254, 49
- 16 T.A. Peters, T. Kaleta, M. Stange, R. Bredesen, *Catalysis Today* **2012**, 193, 8
- 17 O. Iyoha, R. Enick, R. Killmeyer, and B. Morreale, *Journal of Membrane science* **2007**, 305, 77
- 18 D. R. Alfonso, A. V. Cugini, D. S. Sholl, *Surface Science* **2003**, 546, 12
- 19 S.M. Opalka, O.M. Løvvik, S.C. Emerson, Y. She, and T.H. Vanderspurt, *Journal of Membrane Science* **2011**, 375, 96
- 20 S.K. Gade, S.J. DeVoss, K.E. Coulter, S.N. Paglieri, G.O. Alptekin, J.D. Way, *Journal of Membrane Science* **2010**, 378, 35
- 21 C.H. Chen, Y.H. Ma, *Journal of Membrane Science* **2010**, 362, 535
- 22 J. F. Gabitto, and C. Tsouris, *International Review of Chemical Engineering* **2009**, 1, 5, 394
- 23 F. Braun, J.B. Miller, A.J. Gellman, A.M. Traditi, B. Fleutot, P. Kondratyuk, L.M. Cornaglia, *International Journal of Hydrogen Energy* **2012**, 37, 18547
- 24 A.M. Venezia, V. La Parola, V. Nicoli, and G. Deganello, *Journal of Catalysis* **2002**, 212, 56
- 25 S. Fletcher, PhD thesis, University of Birmingham, **2009**
- 26 T.A. Peters, T. Kaleta, M. Stange, and R. Bredesen, *Journal of Membrane Science* **2011**, 383, 124
- 27 B.D. Morreale, B.H. Howard, O. Iyoha, R.M. Enick, C. Ling, and D.S. Sholl, *Industrial & Engineering Chemistry Research* **2007**, 46, 19, 6313
- 28 E. Ozdogan, and J. Wilcox, *Journal of Physical Chemistry B* **2010**, 114, 12851
- 29 M.P. Hyman, B.T. Loveless, J. W. Medlin, *Surface Science* **2007**, 601, 5382
- 30 H. Gao, Y.S. Lin, Y. Li, and B. Zhang, *Industrial Engineering Chemical research*, **2004**, 43, 6920
- 31 C. Ling, D.S. Sholl, *Journal of Membrane Science*, **2007**, 303, 162